STRUCTURAL STUDIES OF MATERIALS FOR HYDROGEN STORAGE

Final Report - **High Resolution SR-PXD**: **01-01-863 Beamline BM01B**

Initial comment

The Physics Department at Institute for Energy Technology has a strong activity on hydrogen storage materials, involving many national and international collaborators. The strong position of the group is to a high degree based on the good access to neutrons for powder neutron diffraction (PND) using the PUS diffractometer at the Institute's own research reactor JEEP II.

Synchrotron power X-ray diffraction (SR-PXD) has proven to be an invaluable supplement to PND due to its superior speed and resolution. The data acquisition times are typically 3 orders of magnitude shorter using the MAR345 image plate at BM01A compared to PUS at JEEP II. This allows in-situ investigations of chemical reactions that we cannot possibly follow with PND. In addition, the very high resolution offered at BM01B enables indexing and space group determination from complex structures where the problem with peak overlapping makes the task unmanageable with PND- or laboratory PXD data. So far, the predictable, long-term access to the beam lines at SNBL through the previous long-term projects 01-01-805 and 01-02-862 has been an invaluable supplement to our neutron diffraction facilities and the rest of our experimental activity.

This report summarizes the results that have been obtained in connection with the project 01-01-863.

The crystal structures of $Tb(BH_4)_3$ and $Er(BH_4)_3$: two novel unsolvated borohydrides

The mechano-chemical reaction between $LiBH_4$ and $TbCl_3$ or $ErCl_3$ in a molar ratio of 3:1 has led to the formation of new compounds. For both reactions the products were determined as LiCl and an additional cubic phase with lattice constants of 11.9 and 11.8 Å respectively, as was determined by laboratory X-ray diffraction. HR-SR PXD measurements at BM01B with a wavelength of 0.5032 Å confirmed the initial findings. The structures were solved by ab initio methods *(FOX)* in space group Pa-3 and were found to be novel, solvent-free rare-earth borohydrides, respectively $Er(BH_4)_3$ and $Tb(BH_4)_3$. Rietveld refinement of the structure model with *GSAS* resulted in the following reliability factors: wR_p = 6.54%, R_p = 4.90% and chi^2 = 3.187 for $Tb(BH_4)_3$; wR_p = 4.38%, R_p = 3.45% and chi^2 = 1.672 for $Er(BH_4)_3$. Soft constraints were applied for the geometry of the $[BH_4]$ units, as well as common isotropic displacement factors for all hydrogen atoms. Figure 1 shows the final state of the refinement procedure for both compounds. Table 1 depicts selected interatomic distances and angles for both compounds.

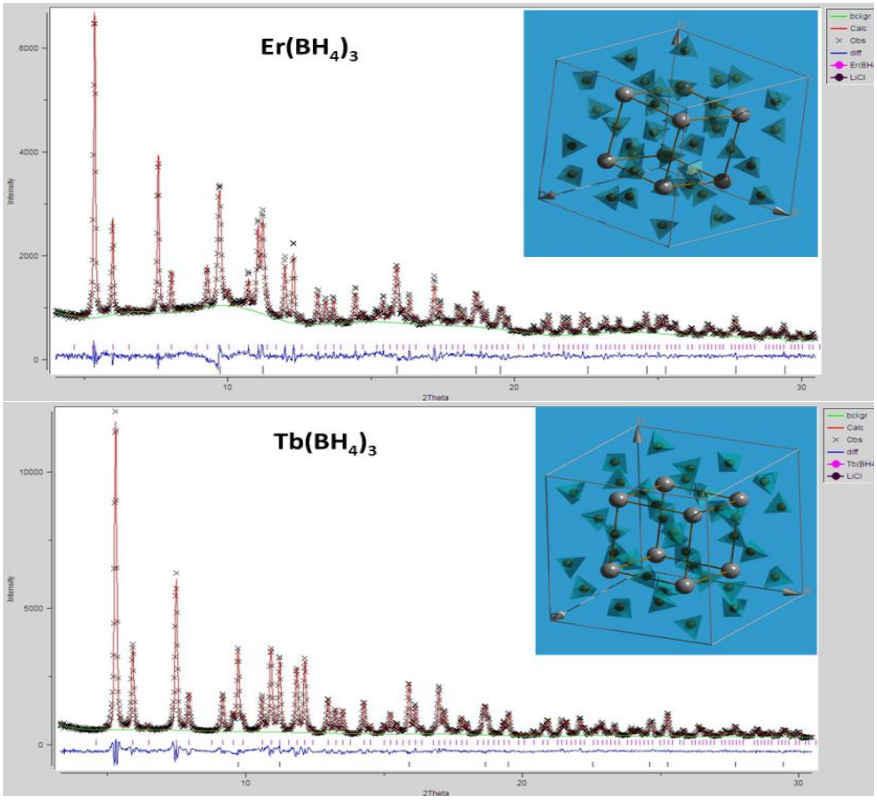

Figure 1: HR-SR PXD data for $Er(BH_4)_3$ and $Tb(BH_4)_3$. The position of Bragg reflections for $Er(BH_4)_3$, $Tb(BH_4)_3$ and LiCl are shown (bars) together with the observed pattern (solid crosses), difference (solid line) and the profile calculated by Rietveld refinement (solid lines). The content of the unit cells is depicted in the inset with Tb and Er as solid spheres and BH_4 units as polyhedra.

(a) $Tb(BH_4)_3$

Phase data	
Space-group	P a -3 (205) - cubic
Cell	a=10.9125(2) Å V=1299.49(8) Å^3 Z=8

Atomic parameters

Atom	Ox.	Wyck.	Site	S.O.F.	x/a	y/b	z/c	U [Å^2]
Tb		8c	.3.		0.78362(8)	0.78362(8)	0.78362(8)	0.0210
B		24d	1		0.7425(19)	-0.0319(15)	0.3011(15)	0.0080
H1		24d	1		0.6719(26)	-0.1070(23)	0.295(4)	0.0203
H2		24d	1		0.768(4)	-0.003(4)	0.2053(20)	0.0203
H3		24d	1		0.8213(23)	-0.058(4)	0.3567(29)	0.0203
H4		24d	1		0.6920(19)	0.0552(18)	0.3426(17)	0.0203

B	H4	1.1116 Å	
	H3	1.1342 Å	
	H1	1.1406 Å	
	H2	1.1432 Å	
B	H4	H3	110.047
	H4	H1	108.051
	H4	H2	114.194
	H3	H1	108.219
	H3	H2	108.656
	H1	H2	107.490
Er	B	3x	2.7147 Å
	B	3x	2.7601 Å

(b) $Er(BH_4)_3$

Phase data	
Space-group	P a -3 (205) - cubic
Cell	a=10.7790(7) Å V=1252.38(23) Å^3 Z=8

Atomic parameters

Atom	Ox.	Wyck.	Site	S.O.F.	x/a	y/b	z/c	U [Å^2]
Er		8c	.3.		0.21580	0.21580	0.21580	0.0120
B		24d	1		0.53399	0.80927	0.73589	0.0200
H1		24d	1		0.57468	0.77232	0.64547	0.0938
H2		24d	1		0.59110	0.89402	0.76426	0.0938
H3		24d	1		0.43509	0.84001	0.71732	0.0938
H4		24d	1		0.53483	0.73269	0.80496	0.0938

B	H3	1.0903 Å	
	H1	1.1268 Å	
	H2	1.1269 Å	
	H4	1.1884 Å	
B	H3	H1	112.467
	H3	H2	113.243
	H3	H4	111.261
	H1	H2	108.518
	H1	H4	106.689
	H2	H4	104.136
Tb	B	3x	2.7310 Å
	B	3x	2.7898 Å

Table 1: Atomic parameters, selected interatomic distances and angles for $Tb(BH_4)_3$ and $Er(BH_4)_3$ crystallizing in space group Pa-3 with a = 10.9125(2) Å and 10.7790(7) Å respectively.

$Tb(BH_4)_3$ and $Er(BH_4)_3$ are both isostructural to α-$Y(BH_4)_3$ and consist of rare-earth ions surrounded by 6 $[BH_4]$ units, resulting in a distorted octahedral environment. The Tb^{3+}/Er^{3+} cations themselves form a distorted cubic arrangement with the $[BH_4]$ units oriented along the cube edges (see Figure 1). The lattice constant for $Tb(BH_4)_3$ is 10.9125(2) Å and lies in between those reported for $Gd(BH_4)_3$ and $Dy(BH_4)_3$, which are 10.983(5) Å and 10.885(3) Å respectively. The lattice constant for $Er(BH_4)_3$ has been determined as 10.7790(7) Å, and is considerably smaller than that found for the Dy, Gd and Er compounds. The reduction in lattice constants (cell volume) for the series of Gd→Tb→Dy→Er borohydrides is a direct consequence of the decreasing ionic radii as a result of the lanthanide contraction. The experimentally determined lattice constants show a linear dependence on the ionic radii of the lanthanide ions, as is expected for a series of isostructural compounds. Both compounds currently await further characterization by Powder Neutron diffraction in order to obtain reliable information about the position of the hydrogen atoms.

The results will be published in a forthcoming article [1].

More on CaB_2H_x: An intermediate obtained from the decomposition of $Ca(BH_4)_2$

A CaB_2H_x phase has previously been identified as an intermediate phase in the decomposition scheme of $Ca(BH_4)_2$ (see final report for long-term project 01-02-772). Based on desorption experiments and difference Fourier mapping of synchrotron radiation powder X-ray diffraction data, the full composition was suggested to be CaB_2H_2, and a structure model was proposed. However, recent theoretical calculations have indicated that the proposed structure is not stable and further investigations are required to verify the structure.

The aim of the experiment carried out at SNBL was to improve that data quality for the high-angle region. Due to the short *b*- and *c*-axes of the unit cell, the 0*kl*, 0*k*0 and 00*l* reflections are scarce in the 2θ region used for indexing and structure determination. Moreover, the phase always forms in a multiphase sample, and the Bragg intensities are relatively weak. A procedure with longer measuring times at higher angles significantly improved the diffraction data quality (Fig. 2).

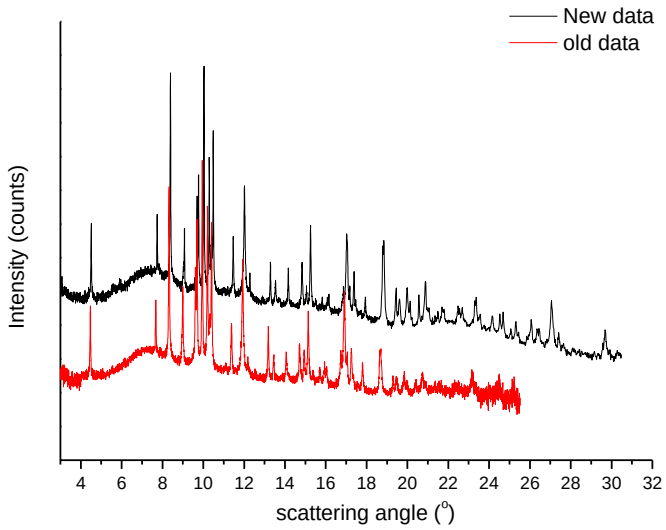

Figure 2: Comparison of previously obtained diffraction data (red) and the new data set (black) measured with increased measuring time at higher angles. The samples are not identical and contain slightly different ratios of CaB_2H_x, CaH_2 and CaO. The data sets are not corrected for a small difference in wavelength.

However, no new information from systematic absences could be obtained, and the data supports the previously reported results. Raman- and IR spectroscopy as well as neutron diffraction experiments have not contributed to further insight, and the next step is to perform elemental analysis using TEM and to continue the analysis on the improved data set.

Formation of a fluorite-type hydride in the Mg-Ti-Co-H system processed by ball milling

Based on thin films studies it has been shown that the Mg-Ti-H system exhibits a high hydrogen storage capacity and a very good electrochemical performance. However, studies on the bulk material have not confirmed such outstanding properties so far.
The synthesis of ternary or/and quaternary hydrogen containing phases with FCC type structure in the Mg-Ti-Co-H system have been performed to study possible Co induced changes in its kinetic and thermodynamic properties.
$(MgH_2)Ti_{0.5}Co_{0.5}$ (Figure 3) and $(MgH_2)_{0.7}(Ti_{0.5}Co_{0.5})_{0.3}$ (Figure 4) powder mixtures were ball milled in a high-energy mill SPEX 8000 under Ar atmosphere. The as-prepared samples were investigated at BM01B.
The HR-SR PXD data show the formation of a fluorite-type structure in both samples. In $(MgH_2)Ti_{0.5}Co_{0.5}$ the fraction of hydrogen containing phase (a = 4.4226(9) Å) accounts for 25 wt.%. Apart from that, the presence of TiCo (75 wt.%) and $TiH_{0.7}$ (5 wt.%) has been confirmed.

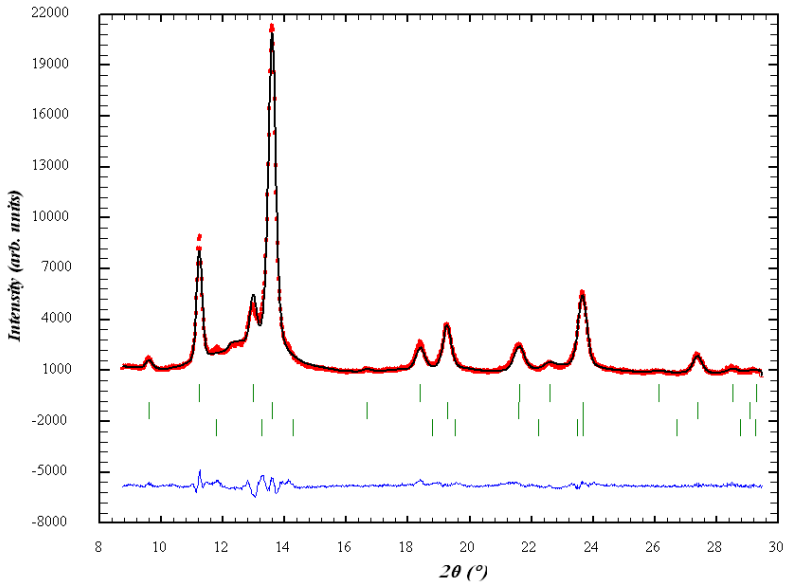

Figure 3: HR-SR PXD data for ball milled $(MgH_2)Ti_{0.5}Co_{0.5}$. The position of Bragg reflections for Mg/TiH_x, TiCo and $TiH_{0.7}$ are shown (bars) together with the observed pattern (solid circles) and the profile calculated by Rietveld refinement (solid lines).

In $(MgH_2)_{0.7}(Ti_{0.5}Co_{0.5})_{0.3}$ the abundance of FCC hydride phase with a slightly bigger unit cell volume (a = 4.427(1) Å) seems higher; however the presence of numerous additional phases hinder the Rietveld refinement significantly. The synthesis conditions need to be optimized in order to eliminate the occurrence of undesired phases and simultaneously retain a high fraction of the hydride.

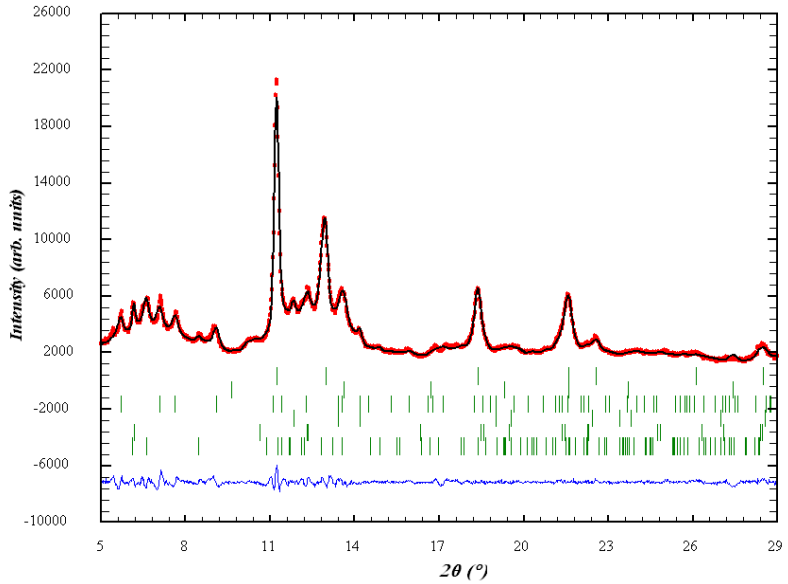

Figure 4: HR-SR PXD data for ball milled $(MgH_2)_{0.7}(Ti_{0.5}Co_{0.5})_{0.3}$. The position of Bragg reflections for Mg/TiH_x, TiCo, Mg_2CoH_5, $TiH_{0.7}$, $Mg(OH)_2$ and TiO_2 are shown (bars) together with the observed pattern (solid circles) and the calculated profile (solid line).

The structural characterization and detailed compositions of both samples will be the subject of further investigations in conjunction with powder neutron diffraction.

Hydride formation in Mg-based systems processed by reactive milling

The possibilities to produce quaternary Mg-based transition-metal complex hydrides have been explored. $Mg_2Mn_{1-x}Fe_x$ (x = 0.5, 0) elemental powder mixtures were ball milled in a reactive D_2 atmosphere (about 5 MPa). The results were compared with the formation of $Mg_2(FeD_6)_{0.5}(CoD_5)_{0.5}$ from Mg-Fe-Co powders.

HR-PXD was previously employed to characterize the as-milled samples, pointing towards the formation of Mg-based transition-metal hydride phases. During subsequent in-situ SR-PXD measurements it was shown that the desorption products were Mg, Fe and an unidentified Mn-based phase. HR-PXD was therefore carried out on fully desorbed samples (after DSC up to 400 °C) in order to investigate in detail the phases formed during deuterium desorption.

As expected, the main desorption products are elemental Mg, Mn and Fe (see Figures 5 and 6). A minor unidentified phase is also observed in the $Mg_2Mn_{0.5}Fe_{0.5}$ sample (Figure 5). Weaker diffraction peaks of the same phase are also observed in the Mg_2Mn sample (Figure 6), which contains a non-negligible amount of Fe due to impurities from the milling process. This suggests that the minor phase contains both Mn and Fe.

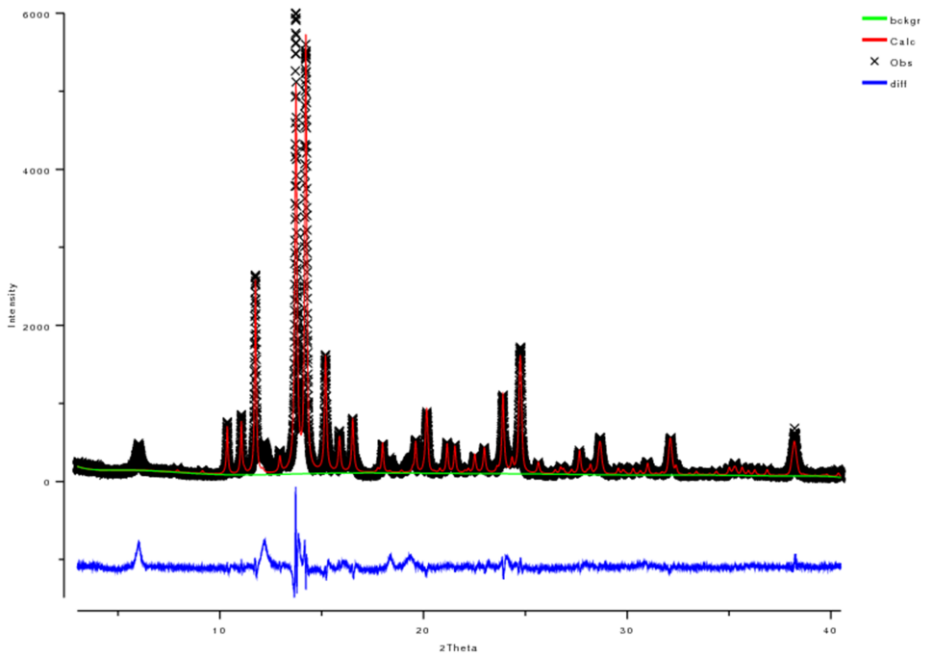

Figure 5: HR-SR PXD data for $Mg_2Mn_{0.5}Fe_{0.5}$ + D_2 after DSC up to 400 °C. The peaks not accounted for in the Rietveld refinement are those for the unidentified Mn-, Fe-containing phase.

A comparison of the HR-SR PXD data with the *in-situ* SR-PXD data is currently being carried out to fully characterize this phase. The results will be presented in forthcoming international conferences.

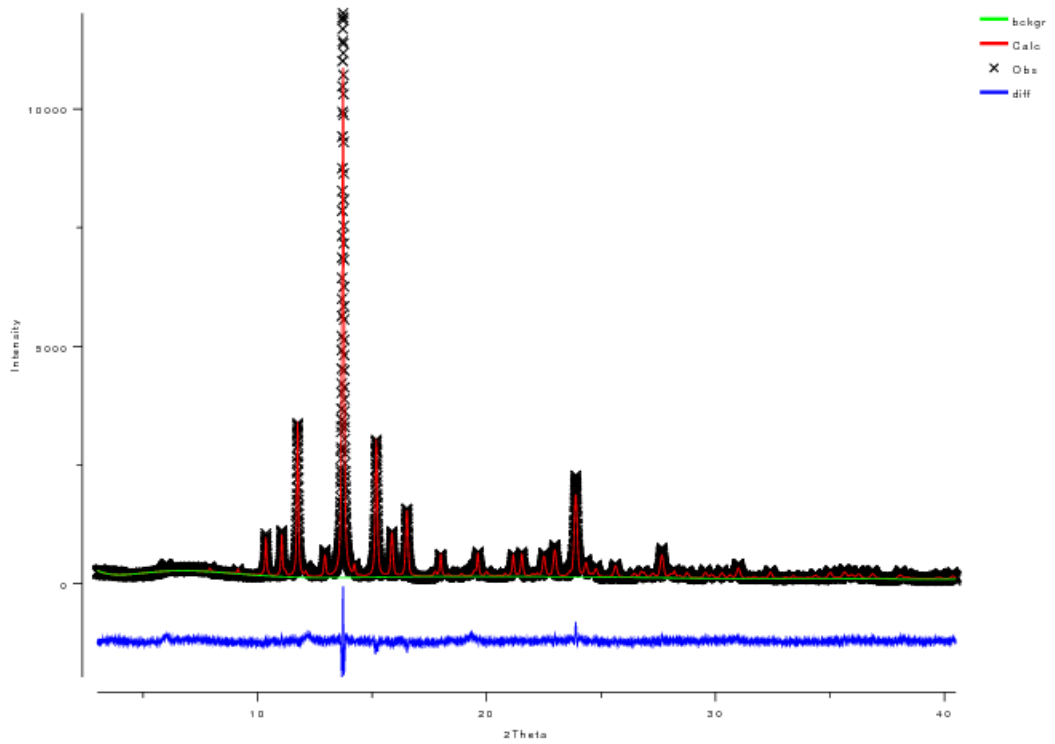

Figure 6: High-Resolution SR-PXD for $Mg_2Mn(Fe)$ + D_2 after DSC up to 400 °C. Weak reflections not accounted for in the Rietveld refinement can be observed.

Magnesium hydride compounds produced by Cryomilling

In spite of its high desorption temperature and slow kinetics, magnesium hydride MgH_2 is still a good candidate for hydrogen storage applications due to its high hydrogen reversible capacity (7.6 wt. %) and low cost. Many studies have shown that doping of MgH_2 with a small amount of additives such as fluorides can decrease the desorption temperature and improve the kinetic properties.

In this work, MgH_2 was mixed with 2 mol % of FeF_3 or NbF_5 and processed by mechanical milling at liquid nitrogen temperature (*cryomilling*). The samples with fluorides presented very fast kinetics and a drastic decrease in desorption temperature. Furthermore, the previous XRD analysis showed a decrease in intensity of the Bragg peaks of β-MgH_2 phase for the samples with fluorides compared to the sample without fluorides. In order to determine if this decrease in intensity was related to the crystallite size reduction, which could also be attributed as a positive effect of the fluoride addition, the samples were measured by HR-SR PXD and later on analyzed by the Rietveld method.

Figure 7 displays the HR-SR PXD patterns for the "MgH_2", "MgH_2+FeF_3" and "MgH_2+NbF_5" samples. The inset in Figure 7 shows that the Bragg peaks of the samples with fluorides are much broader than those of the pure sample. Figure 8 depicts, as an example, the Rietveld refinement applied to the MgH_2 sample. The values for the average crystallite size (*D*) from Rietveld refinement of all samples are shown in table 2. As can be seen, the samples that contain fluoride show a drastic reduction in the

crystallite size compared to samples without fluoride (38,58(6) nm). The average crystallite size for the "MgH_2+FeF_3" sample is 10,89(2) nm while for the "MgH_2+NbF_5" sample is 12,94(4) nm.

The high- resolution SR-PXD analysis followed by the Rietveld method confirmed that during the cryomilling process of MgH_2 the addition of fluorides (FeF_3, NbF_5) can be used to reduce the crystallite size and to improve the kinetic properties.

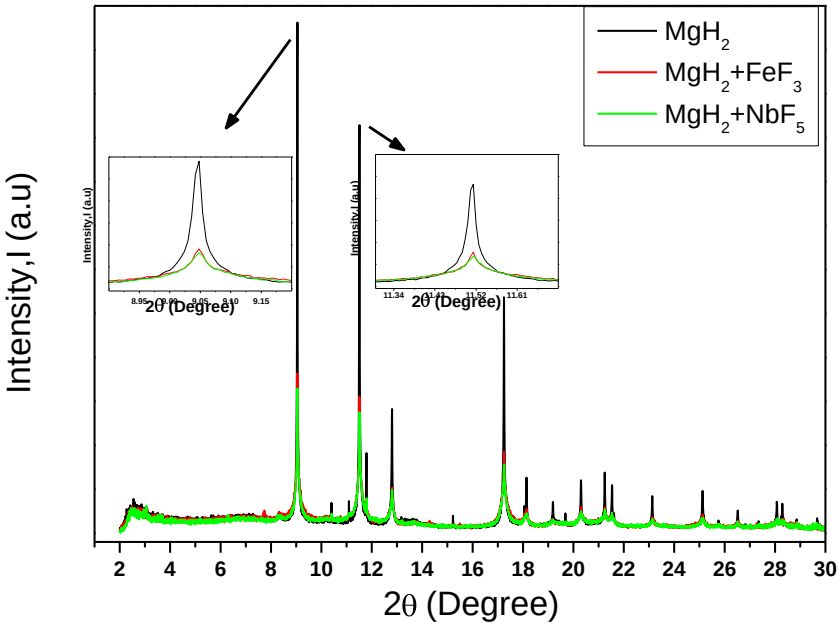

Figure 7: HR-SR PXD patterns for the samples: MgH_2; MgH_2+2 mol % FeF_3 and MgH_2+2 mol % NbF_5.

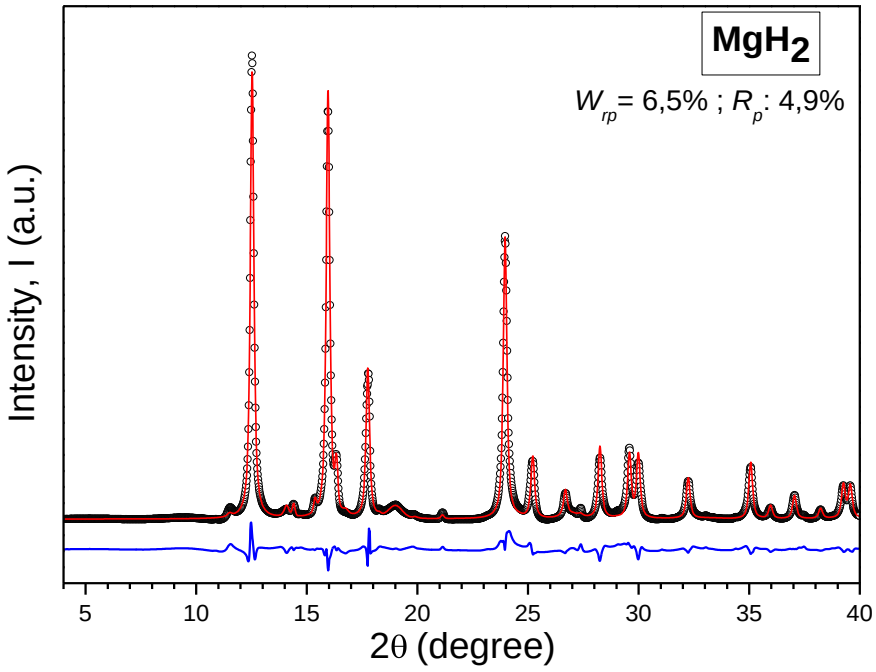

Figure 8: Rietveld refinement profile for MgH_2. Black line: observed pattern; Red line: calculated pattern; Blue line: Difference (residual).

Table 2: Estimated crystallite size obtained by Rietveld method for samples containing MgH_2; "MgH_2+FeF_3" and "MgH_2+NbF_5".

Samples	***D (nm)***
MgH_2	38,58(6)
MgH_2+FeF_3	10,89(2)
MgH_2+NbF_5	12,94(4)

The mechano-chemical reaction between $LiBH_4$ and $YbCl_3$

Ball-milling is a feasible alternative to wet-chemical methods in order to synthesize borohydrides, since it allows preparation of these materials without the need for additional solvents. This eliminates the existence of intermediate solvent-adducts that have to undergo heat-treatment in order to obtain the solvent-free materials.

The mechano-chemical reaction between $LiBH_4$ and $YbCl_3$ in a molar ratio of (3:1) was found to proceed without gas evolution, which indicated that ytterbium was kept in its original trivalent state, and that the reaction was conducted without decomposition of the starting materials.

HR-SR PXD (BM01B) data were collected on samples with different milling times. In addition to the earlier reported phase, with very broad peaks and indexed in a cubic unit cell (space group *P23*, a = 6.2008(8) Å), two new phases have been identified. The sample obtained after 6 hours of milling can be indexed in a cubic unit cell with a = 10.705 Å in space group *Pa-3*. This phase has been identified as isostructural to the reported room-temperature modification of $Y(BH_4)_3$. The sample obtained after 1 hour of milling includes a small amount of a phase that has been identified as isostructural to the reported high-temperature modification of $Y(BH_4)_3$. These phases has been named α-$Yb(BH_4)_3$ and β-$Yb(BH_4)_3$, respectively. β-$Yb(BH_4)_3$ crystallizes in the cubic space group *Fm-3c* with a lattice constant a = 10.883 Å.

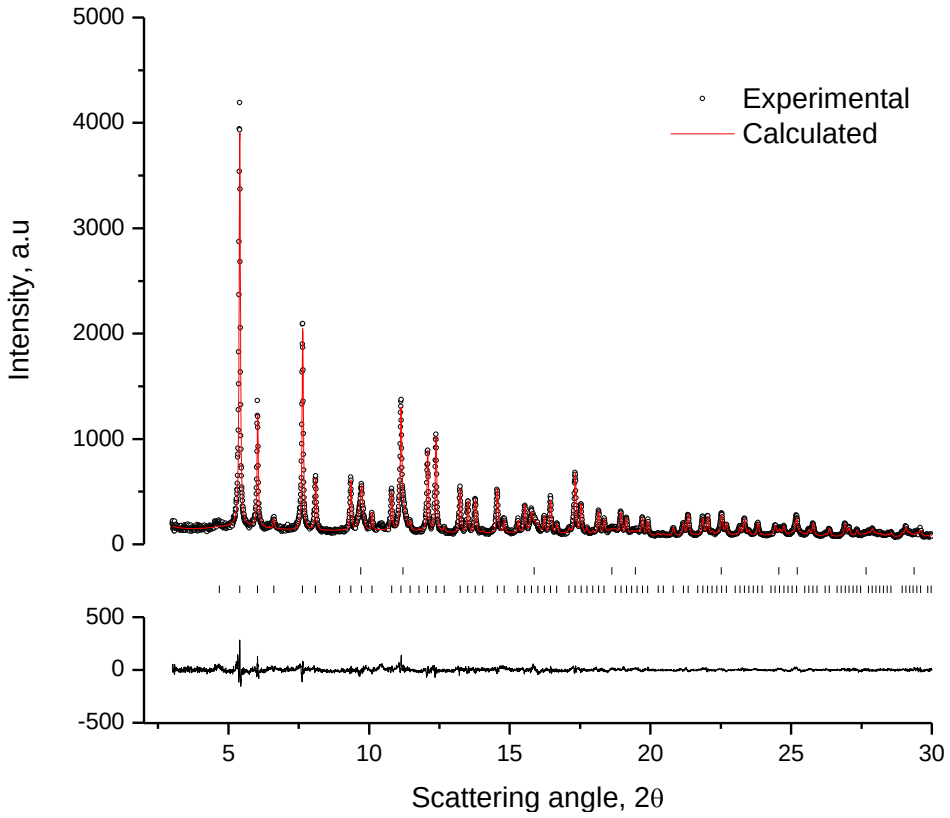

Figure 9: The Rietveld refinement for α-Yb(BH$_4$)$_3$. The experimental data (circles), the calculated diffraction pattern (solid line), tick marks for LiCl (upper) and α-Yb(BH$_4$)$_3$ (lower), and the differential plot (bottom solid line) are shown.

The results will be part of a forthcoming publication [2].

Concluding remarks

HR-SR PXD measurements at SNBL station BM01B, in connection with the project 01-01-863 have led to the discovery of a series of new compounds and structures. The data analysis is still on going and it is planned to submit at least 2 papers during the year 2012 based on the results obtained so far.

References

[1] Frommen C, Sørby M.H. and Hauback B.C. "Crystal structure and thermal properties of Er(BH$_4$)$_3$ and Tb(BH$_4$)$_3$", preparation in progress

[2] Olsen J.E., Frommen C, Sørby M.H and Hauback B.C. "Structure, polymorphism and thermal decomposition of Yb(BH$_4$)$_3$", preparation in progress